Journal of Alloys and Compounds 253–254 (1997) 629–634

The recent research, development and industrial applications of metal hydrides in the People's Republic of China

Q.D. Wang*, C.P. Chen, Y.Q. Lei

Department of Materials Science and Engineering, Zhejiang University, Hangzhou, Zhejiang 310027, P.R. China

Abstract

Chief accomplishments in the research and development of hydrogen storage alloys and hydride technology in recent years in the People's Republic of China are summarized and reported.

Keywords: Hydrogen storage intermetallics; Metal hydrides; Hydride technology; Metal hydride applications

1. Introduction

The national policy of the People's Republic of China for the advancement of science and technology demands the research and development of application orientated projects to serve directly the development of national economy. This policy has made the R&D of metal hydrides focus on some applications with market prospects including, hydride hydrogen storage, recovery, purification, compression, transportation, hydride heat pumps, vehicular applications, hydride catalysts, electrode alloys and nickel/metal hydride batteries. The present paper is arranged according to these items.

2. Hydride hydrogen storage

The first achievement in P.R.C in hydride technology was the development of hydrogen storage alloy $MlNi_5$ used for hydride hydrogen storage by Zhejiang University [1]. Ml, a byproduct in the extraction of Ce, is called in China the La-rich mischmetal while Mm is used to designate Ce-rich mischmetal as shown in Table 1.

The thermodynamic and kinetic properties of $MlNi_5$ are quite similar to those of $LaNi_5$. As Ml is a cheap byproduct in Ce extraction, the price of $MlNi_5$ is only 40% that of $LaNi_5$. In comparison with $TiFe_{0.9}Mn_{0.1}$, $MlNi_5$ has a better antipassivation property and a more flat plateau pressure and is hence preferred to TiFe based alloys by users. Storage containers of 2, 6, 12, 30 and 80 m^3 (under standard conditions) have been built for laboratories, hybrid cars and factories by Zhejiang University and other institutions. Containers over 6 m^3 are usually composed of tubes filled with 2~5 wt.% of Al fiber to prevent the tubes from swelling damage and incased in water jackets for heating or cooling and are illustrated in Fig. 1.

A storage container can easily be converted into a suprapure hydrogen purification unit refining industrial hydrogen (98% purity) into hydrogen of 99.9999% purity with dewpoint below −80 °C when a molecular sieve pretreatment unit is used firstly to remove moisture and oxygen impurities from the incoming gas, since $MlNi_5$ has

Fig. 1. The hydride container of 80 m^3 (under standard conditions) hydrogen capacity.

---

*Corresponding author.

0925-8388/97/$17.00
PII S0925-8388(96)02977-5

Table 1
The compositions of mischmetals

Kinds of mischmetal	Symbol	Composition (wt.%)			
		La	Ce	Pr	Nd
La-rich mischmetal	Ml	44–51	3–5	9–11	24–41
Ce-rich mischmetal	Mm	20–30	45–52	5–8	13–20

a high catalytic activity for combining hydrogen with oxygen to form water, which condenses on the alloy particles and container walls and thus becomes very difficult to be blown out [2]. For the sake of conserving high purity hydrogen used in blowing off gaseous impurities concentrated in the container after hydriding, an extra outlet valve is installed on the other end of the container from the inlet valve to allow the incoming gas to carry away most of the concentrated gaseous impurities [3].

3. Hydride hydrogen recovery, purification storage and transportation

Scientists of Zhejiang University developed two series of Mn and Al substituted low plateau pressure mischmetal–nickel hydrogen storage alloys [4] for the recovery of hydrogen from waste gases. The alloy $MlNi_{4.9}Al_{0.1}$ is often adopted for the recovery of hydrogen from either the purge gas or the feed gas of synthetic ammonia production. In one application, hydrogen is absorbed into big double valve containers in an ammonia plant, then desorbing hydrogen is used to blow the remaining hydrogen to high purity and the containers are transported to consumers on trucks or trailers. This process has been proven to be meritorious economically, environmentally and in safety aspects. The scheme of the processes is shown in Fig. 2 and a truck load of hydride containers (320 m^3 hydrogen under standard conditions) supplying high purity hydrogen to a float glass plant is shown in Fig. 3 [5].

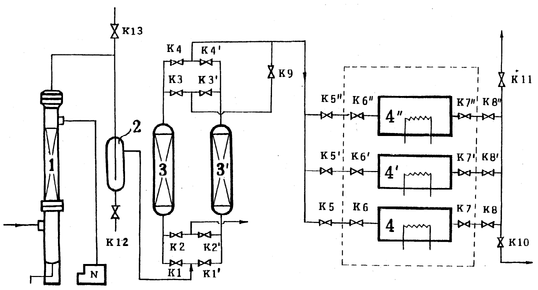

Fig. 2. The schematic diagram for the process of recovering hydrogen from the purge gas of an ammonia plant and subsequent purifying and transporting in hydride tanks. (1) ammonia wash tower, (2) gas water separator, (3) (3′) gas dryers, (4) (4′ 4″) hydride hydrogen recovery, purification and transportation tanks, K_1 (K_2, K_3 ⋯ ⋯) valves [5].

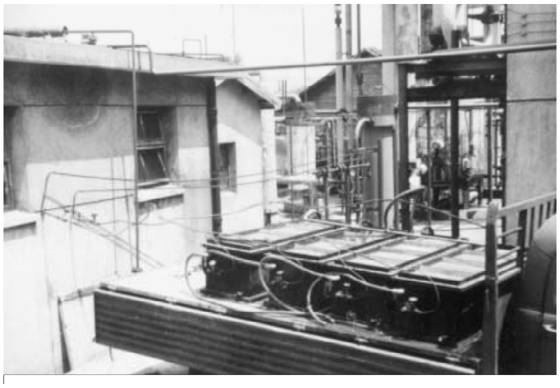

Fig. 3. Four hydride containers (80 m^3 each) loaded on a truck for hydrogen recovery, purification, storage and transportation [5].

4. Hydride hydrogen compression

According to the thermodynamic properties of hydrides the desorption pressure of a hydride bed varies with its temperature according to van Hoff's equation

$$\ln P_d = \frac{\Delta H^0}{RT} - \frac{\Delta S^0}{R}.$$

When a hydride bed is made to absorb hydrogen at a lower temperature T_l and desorb at a higher temperature T_h, the pressure ratio R can be expressed as

$$R = \exp\left[\frac{\Delta H^0}{R}\left(\frac{1}{T_h} - \frac{1}{T_l}\right)\right] - \frac{\Delta P_{ad}(T_h)}{P_d(T_l)}$$

where $\Delta P_{ad}(T_h)$ is the hysteresis pressure differential at temperature T_h, and $P_d(T_l)$ is the desorption pressure at temperature T_h. To obtain a large R for two definite temperatures, one must make ΔH^0 large and $\Delta P_{ad}(T_l)$ small. Conforming to the requirement of using steam heating instead of electric heating in small factories in China, we usually choose $T_l = 293$ K and $T_h = 373$ K. For inlet hydrogen with sufficiently high pressure (say 2.5 MPa or higher) a one stage compression unit is sufficient to compress hydrogen to 15 MPa, to fill gas cylinders. On the other hand, if the inlet gas pressure is rather low (say 0.5 MPa or lower) a two stage compression is usually required [6]. Multicomponent alloys were also developed by Zhejiang University for both pressure stages [7].

A compressor can also be used as a purifier when the incoming gas is first made to pass through a molecular sieve pretreatment unit to remove oxygen and moisture. The purity of hydrogen from a purifying–compressing unit can also reach 99.9999%. Two purifying–compressing units are shown in Fig. 4 and Fig. 5.

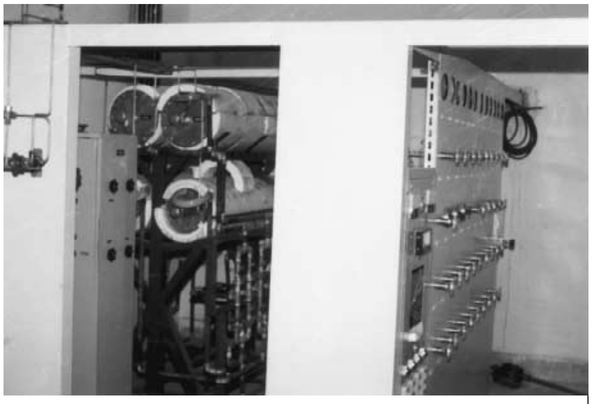

Fig. 4. A 12 m^3/h suprapure hydrogen two stage hydride compressor using feed gas from an ammonia plant.

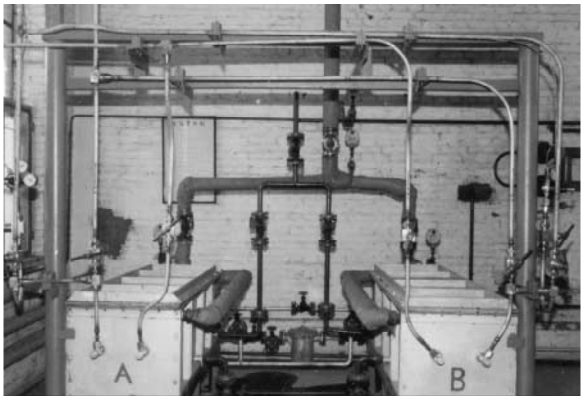

Fig. 5. A 24 m^3/h suprapure hydrogen single stage compressor with two tanks for continuous hydrogen supply.

5. Vehicular application

For the sake of developing environmentally cleaner city buses, Zhejiang University developed a new hydrogen storage alloy, a new hydride hydrogen storage tank and a new hydrogen injection technology. They investigated systematically the $Ml_{1-x}Ca_xNi_5$ alloy series and found $Ml_{0.8}Ca_{0.2}Ni_5$ to have the best overall properties. The alloy is comparatively light in weight and has a desorption pressure of 1.0 MPa at 25 °C and a large storage capacity, attaining 1.62 wt.% H_2 (185 ml/g) hence suitable for vehicular hydrogen storage. Fig. 6 shows the test minibus, in the engine of which a microprocessor actuated high speed valve is used for hydrogen injection to control back-fire. This minibus runs smoothly. When 4.7 wt.% hydrogen is used together with gasoline, a 40% conservation of gasoline is realized. The heat efficiency is increased by 14% and CO and NO_x are lowered by 70% in emission.

Fig. 6. The 19 seater gasoline hydrogen hybrid powered minibus.

6. Hydride heat pumps

As a part of the national high technology development plan, Zhejiang University has been engaging also in the development of hydride heat pumps. Currently they are working on a test air conditioning unit for a 40 seater bus. The refrigerating capacity is designed at 12 000 kcal h^{-1} in summer and a heating capacity of 16 000 kcal h^{-1} in winter. The exhaust gas is the source of heat. The temperature regime is taken as 150~250 °C/35~50 °C/15~25 °C. A newly developed alloy pair $LaNi_{4.55}Cu_{0.30}Al_{0.15}/Mm_{0.80}La_{0.20}Ni_{4.35}Fe_{0.65}$, in which both alloys have flat and long plateau pressures and small pressure hysteresis, is employed for the refrigerating cycle. Fig. 7 shows the cycle on the van't Hoffs diagram of the

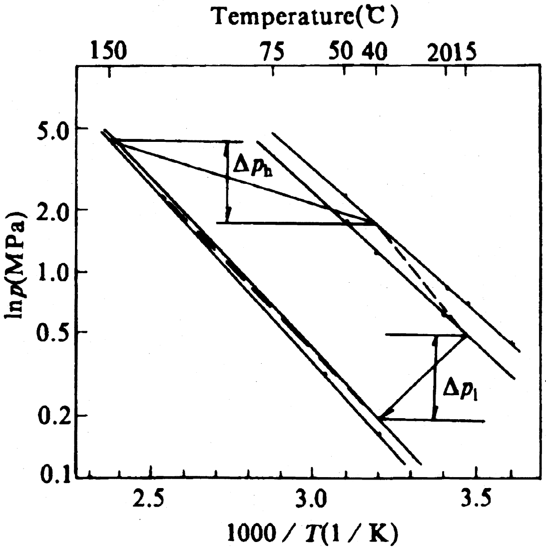

Fig. 7. A refrigeration cycle on the van't Hoffs plot of the $LaNi_{4.55}Cu_{0.30}Al_{0.15}/Mm_{0.60}Ml_{0.20}La_{0.20}Ni_{4.35}Fe_{0.65}$ pair.

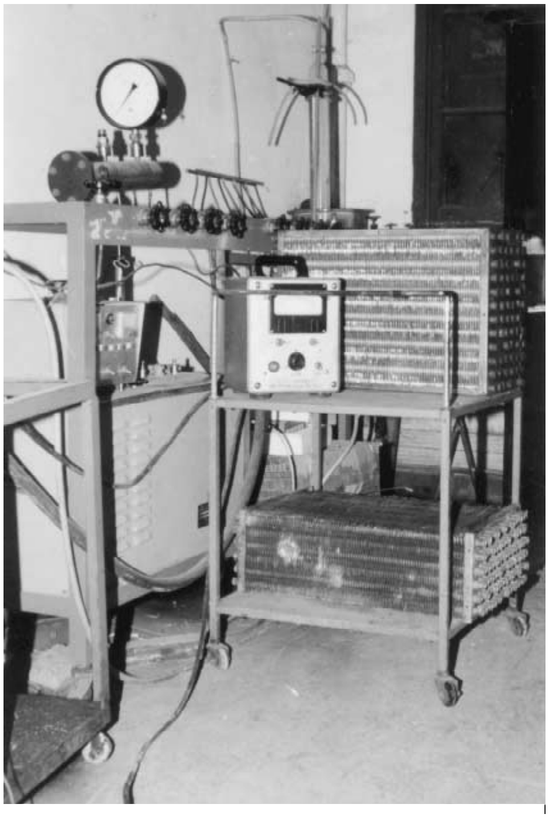

Fig. 8. The photograph of the 1:4 model heat exchanger.

pair of alloys at 150 °C/40 °C/15 °C. The effective hydrogen capacities of the pair are $\Delta C_{h,max} = 4.0\sim4.2$ H/M and $\Delta C_{l,max} = 4.1\sim4.4$ H/M. The calculated $COP_c = 0.61$.

Fig. 8 is the photograph of a 1:4 model heat exchanger, which consists of 78 pieces of ∅10×550 mm copper tubes equipped with 0.2 mm thick Al external fins. Into the tubes of each heat exchanger 25 kg of alloy and 1 kg of Al fiber are loaded. The heat exchanger is claimed to have good heat exchange properties.

7. Hydrogenation catalysts

Recently in Zhejiang University, on the basis of a series of studies on hydrogenation of oleic acid into stearic acid in batch reactors over $LaNi_{4.8}Cu_{0.2}$ or its hydride $LaNi_{4.8}Cu_{0.2}H_{4.5}$ powder as catalyst, they discovered that the hydrogen desorbing from the $LaNi_{4.8}Cu_{0.2}H_{4.5}$ was the chief source of hydrogen for hydrogenation. On the basis of this result, they designed and constructed a tubular reactor for continuous hydrogenation of oleic acid under moderate conditions. As shown in Fig. 9, the reactor consisted of two concentric pipes. The inner one was a porous sintered stainless steel tube with a layer of $LaNi_{4.8}Cu_{0.2}$ powder (0.8~1.0 mm thick) compacted and sintered on its surface. The outer tube was a regular stainless steel pipe. The whole setup was immersed in a water bath kept at 90 °C. During testing, oleic acid was made to flow through the outer pipe and hydrogen to flow through the inner. While flowing, hydrogen diffused through the porous wall first to the catalyst layer and transformed the intermetallic compound into its hydride, and also a small part of hydrogen entered the liquid directly. This part of hydrogen made the liquid layer close to the surface turbulent. Over the interface between metal hydride and liquid, continuous hydrogenation of oleic acid was being carried out. As atomic hydrogen on the interface of the catalyst was consumed by the oleic acid, it was quickly replenished by diffusion through the metal hydride with higher hydrogen concentration in the vicinity. This continuous system proved to be very efficient. Not only can the hydrogenation be carried out at lower temperature and pressure (90 °C and 0.5 MPa) but the rate of conversion is 15 to 20 times faster in comparison with that in a batch reactor over Rainy nickel as catalyst at the same temperature and 1.5 MPa hydrogen pressure [8].

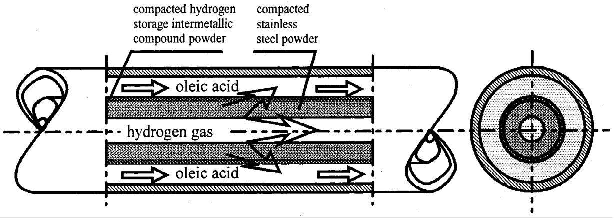

Fig. 9. Structure of the continuous tubular hydrogenation reactor.

8. Hydrogen storage electrode alloys and Ni/MH battery

Zhejiang University started to investigate the $MlNi_5$-based electrode alloys in 1985. They claimed that the alloy $MlNi_{3.8}Co_{0.75}Mn_{0.40}Ti_{0.05}$ had an initial discharge capacity of 260~280 mAh g^{-1} and good overall properties [9]. To commercialize the alloy, Zhejiang University developed the hydrogen decrepitation technique for pulverizing the alloy ingots and the microencapsuluting technology for improving further the cycle life of the alloy. Fig. 10 shows the hydrogen decrepitation unit. Alloys are first crushed into lumps of 10 to 20 mm diameter and loaded into stainless steel tubes into which ultrapure hydrogen is then admitted for hydriding, dehydriding occurs afterwards by heating to a high temperature. Alloy powder thus prepared has a good activation property, and good grain size distribution. Particles with size less than 500 mesh can be controlled to within 6%. Micro-encapsulating the powder with 10 to 15 wt.% of Ni through electrodeless plating increases, evidently, the cycling life and improves also the electric conductivity and surface activity of the alloy powder.

The overall properties of the aforesaid alloy were further

Fig. 10. The hydrogen decrepitation unit for pulverizing the hydrogen storage electrode alloy.

elevated by means of optimizing the constituents of rare-earth elements in mischmetals. A systematic study on the effect of chief constituents of rare-earth ($Re=La_{1-x-y-z}Ce_xNd_yPr_z$) in $ReNi_{3.8}Co_{0.75}Mn_{0.4}Ti_{0.05}$. A series of plots, such as the one shown in Fig. 11, was made to indicate the variation of electrochemical properties with the composition of Re [10]. From the result of optimization when $Re=La_{0.4}Ce_{0.1}Nd_{0.2}Pr_{0.3}$, the maximum electrochemical capacity reaches 290 mAh g^{-1}. When the two most common rare-earth metals in China are adopted, combined and correctly proportioned, the maximum capacity of 280 mAh g^{-1} can be reached with $Re=Ml_{0.85}Mm_{0.15}$. Similar results can also be obtained when rare-earths with different compositions are used, on the condition that they are well proportioned. Properties of nonstoichiometric alloys have also been studied.

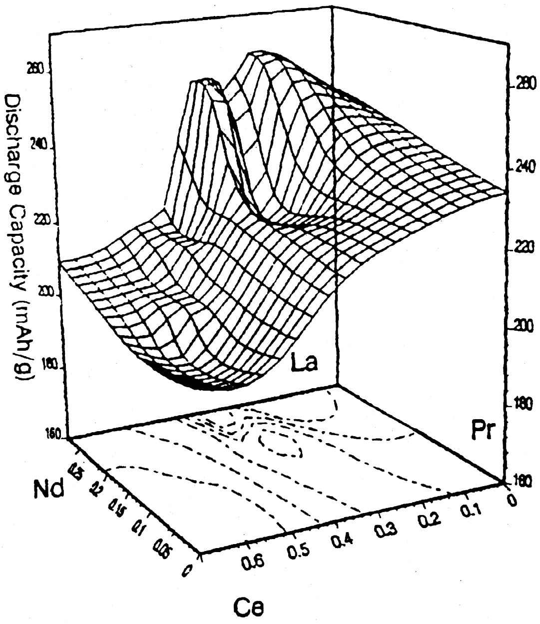

Fig. 11. The variation of electrochemical discharge capacity of the alloy $ReNi_{3.8}Co_{0.75}Mn_{0.40}Ti_{0.05}$ with Re ($Re=La_{0.7-x}Ce_xNd_yPr_{0.3-y}$ and $x=0\sim0.7$, $y=0\sim0.3$).

Systematic studies on Zr-based Laves phase alloys have also been conducted by Zhejiang University. One is the $Zr(Cr_xNi_{1-x})_2$ series with $0.15\leq x\leq0.65$. They found the alloy $Zr(Cr_{0.35}Ni_{0.65})_2$, mainly in C15 Laves phase structure, to have a maximum electrochemical discharge capacity of 305 mAh g^{-1} at 298 °C with a long cycle life, and its activation process can be accelerated by immersing in $HF–H_2O$ solution [11]. They also investigated the $Zr(Mn_xCr_yV_zNi_{1-x-y-z})_2$ series and found the alloy $Zr(Mn_{0.35}Cr_{0.08}V_{0.02}Ni_{0.65})_2$ to have a maximum capacity of 375 mAh g^{-1} with cubic C15 and hexagonal C14 Laves phase as the main phases and six minor coexisting phases such as orthorhombic Zr_7Ni_{10} and tetragonal Zr_9Ni_{11} [12]. Also a study on the crystal structure, phase abundance and thermodynamic properties of $Zr(Mn_{1-x}Ni_x)_2$ $(0.40\leq x\leq 0.75)$ were systematically conducted.

Zhejiang University has also been engaging in the study of the electrochemical behaviors of some amorphous $Mg_{50}Ni_{50-x-y}M_xN_y$ (M, N=Co, Al and Si) hydrogen storage alloys prepared by mechanical alloying. It was found that each mechanically alloyed amorphous alloy reaches its maximum capacity at the first charge/discharge cycle and $Mg_{50}Ni_{50}$ has a maximum discharge capacity around 500 mAh g^{-1}, which is almost ten times higher than that of the same alloy in the crystalline state. However, the durability of the amorphous MgNi-based alloys is very poor, with a degradation rate of 10~60 mAh g^{-1} per cycle. They probably can serve only special purposes [13,14].

Many other institutions have developed their own rare-earth-based electrode alloys; Nankai University claimed the alloys $MmNi_{3.8}Co_{0.5}Mn_{0.4}Al_{0.3}$ and $MmNi_{3.8}Co_{0.5}Mn_{0.3}Al_{0.2}Li_{0.2}$ [15] to be good alloys. They believe that the active element Li has a strong surface catalytic activity, which accelerates the recombination of O_2 and H_2 generated during cell reactions, and hence lowers the internal pressure of hermetic cells and increases their cycle lives [16].

Aiming at alloys with lower prices, the Beijing General Institute for Non-ferrous Metals recommends $MlNi_{3.3}Al_{0.7}Cu_{0.5}Co_{0.2}$ and $MlNi_{3.4}Al_{0.4}Cu_{0.3}Si_{0.2}$ with low Co or no Co [17]. Aiming also at low Co or no Co alloys, Beijing University of Science and Technology made systematic studies on Mm–Ni–Cu–Al and Ml–Ni–Co–Cu–Al alloys and reported $MmNi_{3.45}Co_{0.75}Al_{0.8}$ and $MlNi_{3.5}Co_{0.5}Cu_{0.2}Al_{0.8}$ as being effective [17].

With respect to AB_2 Laves phase alloys, Nankai University studied the Zr-based non-stoichiometric alloys and recommended the alloy $Zr(V_{0.2}Mn_{0.2}Ni_{0.6})_{2.4}$ as a good one with wide plateau region and reasonably flat plateau pressure and initial discharge capacity around 320 mAh g^{-1}. For improving the electrocatalytic activity and the activation behavior of the alloy electrode, HF acid solution treatment (pH 1.5~2.5, 15 min.) was made. The electrocatalytic activity of the alloy was significantly improved due to the removal of the passive ZrO_2 surface layer.

Zhejiang University, Nankai University, Tsinghau University, Shanghai Technical University, the Beijing General Institute for Non-ferrous Metals, Beijing General Institute for Iron and Steel, the Institute of Metals of the Academy of Sciences of China and many other institutions are all affiliated with some factories for alloy and battery production. The total capacity of alloy production in China in 1995 was estimated at around 1000 tons/year, all made in vacuum induction furnaces, ranging from 25 kg/batch to 200 kg/batch. $MlNi_5$-based and $MmNi_5$-based alloys are used for battery manufacturing. Ni- or Cu-coated powder and powder with no coating are all produced. The total annual productivity of Ni/MH batteries is estimated to be 30 million Ah from some 30 factories. There are 5 bigger factories, with annual productivity of 10 million Ah each are now under construction. There is not a lot of difference in the qualities of the batteries from the different factories. The performance of a typical AA size battery is as follows: electrochemical capacity 1100~1200 mAh cycling life$>$500 cycles; 28 days self discharge$<$30% [18].

References

[1] C.P. Chen, J. Wu and Q.D. Wang, *Rare Earth, 3* (1984) 8–13 (in Chinese).
[2] Q.D. Wang, J. Wu, C.P. Chen, W.F. Lou and T.S. Fang, *Hydrogen Energy Progress VI*, Pergamon Press, NY, 1986, pp. 881–886.
[3] Q.D. Wang, J. Wu, C.P. Chen, M. Au and T.S. Fang, *Hydrogen Energy Progress VI*, Pergamon Press, NY, 1986, pp. 872–880.
[4] Q.D. Wang, J. Wu, C.P. Chen and Z. Ye, *J. Less-Common Met., 131* (1987) 321–328.
[5] M. Au, C.P. Chen, Z. Ye, T.S. Fang, J. Wu and Q.D. Wang, *Int. J. Hydrogen Energy, 21* (1996) 33–37.
[6] C.P. Chen, Z. Ye, J. Wu and Q.D. Wang, *Z. Phys. Chem., 183* (1994) 251–258.
[7] Q.D. Wang, J. Wu and C.P. Chen, *Z. Phys. Chem., 164* (1989) 1293–1304.
[8] G.M. Zhu, Y.Q. Lei, Q.D. Wang and X.G. Yang, *J. Alloys Comp., 253–254* (1997) 590–593.
[9] Y.Q. Lei, Z.P. Li, C.P. Chen, J. Wu and Q.D. Wang, *J. Less-Common Met., 172–174* (1991) 1265–1272.
[10] Y.Q. Lei, J.J. Jiang, D.L. Sun, J. Wu and Q.D. Wang, *J. Alloys Comp., 231* (1995) 553–557.
[11] Y.Q. Lei, X.G. Yang, J. Wu and Q.D. Wang, *J. Alloys Comp., 231* (1995) 573–577.
[12] J.Y. Yu, Y.Q. Lei, C.P. Chen, J. Wu and Q.D. Wang, *J. Alloys Comp., 231* (1995) 578–581.
[13] Y.Q. Lei, Y.M. Wu, Q.M. Yang, J. Wu and Q.D. Wang, *Z. Phys. Chem., 183* (1994) 141–147.
[14] D.L. Sun, Y.Q. Lei, W.H. Liu, J.J. Jiang, J. Wu and Q.D. Wang, *J. Alloys Comp., 231* (1995) 621–624.
[15] US Patents 5 242 656, 1993.
[16] US Patents 5 354 576, 1994 and 5 358 800, 1994.
[17] L.J. Jiang, F. Zhan, D.Y. Bao, G.R. Qing, Y.Q. Li and X.Y. Wei, *Energy Storage Materials and Nickel/Metal Hydride Batteries*, Published by National High Technology New Energy Storage Materials Center of China, 1996, pp. 62–66 (in Chinese).
[18] W.K. Zhang, J.G. Hao, Y. Hao, Q.S. Duan and W.S. Li, *Energy Storage Materials and Nickel/Metal Hydride Batteries*, Published by National High Technology New Energy Storage Materials Center of China, 1996, p. 105. (in Chinese).